Carbohydrate Polymers 92 (2013) 394–399

Contents lists available at SciVerse ScienceDirect

Carbohydrate Polymers

journal homepage: www.elsevier.com/locate/carbpol

Determination sulfamethoxazole based chemiluminescence and chitosan/graphene oxide-molecularly imprinted polymers

Qiu Huamin[a,b], Fan Lulu[a,b], Xiangjun Li[a,b], Leilei Li[a,b], Sun Min[a,b], Luo Chuannan[a,b,*]

[a] *School of Chemistry and Chemical Engineering, University of Jinan, No. 106, Jiwei Road, Jinan 250022, China*
[b] *Key Laboratory of Chemical Sensing & Analysis in Universities of Shandong, University of Jinan, Jinan 250022, China*

ARTICLE INFO

Article history:
Received 30 May 2012
Received in revised form 30 August 2012
Accepted 28 September 2012
Available online 6 October 2012

Keywords:
Flow injection chemiluminescence
Chitosan
Graphene oxide
Molecularly imprinted polymers
Sulfamethoxazole

ABSTRACT

A novel flow injection chemiluminescence (FI-CL) sensor for the determination of sulfamethoxazole (SMZ) was established which using chitosan/graphene oxide-molecularly imprinted polymers (CG-MIP) as recognition element. The SMZ-CG-MIP was synthesized in acetone as solvent and chitosan/graphene oxide for support, using acrylamide as functional monomer, ethylene glycol dimethacrylate as cross-linker and 2,2-azobisisobutyronitrile as initiator. The CG-MIP showed satisfactory recognition capacity for the SMZ. Then the synthesized CG-MIP was employed as recognition by packing into a lab-made tube connected in FI-CL analyzer to establish a novel CL sensor respectively. The CL intensity responded linearly to the concentration of SMZ in the range 1.0×10^{-7} mol/L to 2.3×10^{-3} mol/L with a detection limit of 2.9×10^{-8} mol/L (3σ), which is lower. The relative standard deviation for the determination of 4.0×10^{-4} mol/L of SMZ was 1.92% ($n = 11$). The sensor is reusable and has a great improvement in sensitivity and selectivity for CL analysis which applied to the determination of SMZ in drug samples.

1. Introduction

Graphene has attracted considerable attention in recent years for its two-dimensional structure and extraordinary properties (Novoselov et al., 2004). This unique nanostructure holds great promise for potential applications in nanomaterials and nanotechnology (Ying, Xin, Cunku, Jingyao, & Xijiang, 2010). So far, chemical modification and functionalization of graphene has focused on incorporating graphene sheets in a composite material (Mingyu et al., 2011; Park et al., 2008; Stankovich et al., 2006; Veca et al., 2009). Recently, molecular imprinting technology (MIT) is a highly accepted tool for the preparation of tailor-made recognition material, with cavities that are able to selectively recognize a target molecule (Englert et al., 2009; Mahony, Nolan, Smyth, & Mizaikoff, 2005). However, molecularly imprinted polymers (MIP) prepared by the conventional technique has some disadvantages such as low-adsorption capacity. In recent years, to overcome these drawbacks, a large surface area and high porosity 3D platform as graphene, for MIP have been developed (Yan, Yu, Shiyu, Fenghua, & Li, 2011). The following characteristics of graphene make it possible to increase the sensitivity and improve the binding kinetic properties such as strictly two-dimensional material; large surface area; high surface-to-volume ratio (Ying et al., 2010). Since graphene oxide (GO) can be dispersed at the individual sheet level in water, it is possible to achieve a truly molecular-level dispersion of GO if water is used as the common solvent for both GO and the polymer matrix. In addition, it has been reported that the epoxy groups in GO favor to react with primary amine group by addition, which has been widely used to modify GO. So it is possible to form a new mixture of chitosan (Cs) and GO through the special interaction beside the H-bondings between them (Donglin, Lifeng, Wufeng, & Wan, 2011).

Flow injection chemiluminescence (FI-CL) is known as a powerful analytical technique for providing convenient operation, rapid and accurate determination (Luaces et al., 2011). However, the poor selectivity limits its further development and application (Zeng, Yang, Wang, Li, & Qu, 2011). The molecularly imprinted technology was introduced into CL analysis for improving selectivity by its high selective recognition and capture capabilities (Du, Shen, & Lu, 2003). Molecularly imprinted polymers are polymers prepared in presence of template that serves as mould for the formation of template-complementary binding sites (Du et al., 2003). To produce molecularly imprinted polymers two different approaches have been developed: the set up of covalent interactions between template molecules and monomers (Mosbach, 1994a, 1994b) and the development of reversible non-covalent interactions (mainly hydrogen bonding) between them (Wulff, Heide, & Helfmeier, 1986). The application of molecularly imprinted materials obtained by this method for the realization of devices for affinity separation, antibody binding and enzyme mimics, biomimetic sensors, has

---

* Corresponding author at: School of Chemistry and Chemical Engineering, University of Jinan, No. 106, Jiwei Road, Jinan 250022, China. Tel.: +86 531 89736065.
E-mail address: chm_luocn@ujn.edu.cn (L. Chuannan).

0144-8617/$ – see front matter © 2012 Elsevier Ltd. All rights reserved.
http://dx.doi.org/10.1016/j.carbpol.2012.09.092

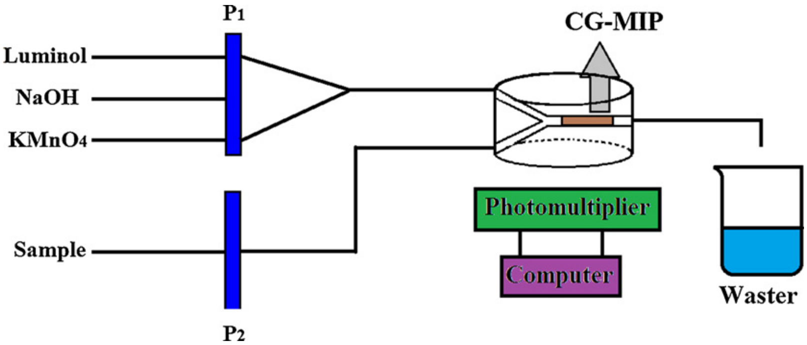

Fig. 1. The schematic diagram of CG-MIP-CL-sensor.

been extensively reviewed (Mosbach, 1994a, 1994b; Mosbach & Ramstrőm, 1996; Shea, 1994; Steinke, Sherrington, & Dunkin, 1995; Wulff, 1995) while recent developments and perspective area evolution excellently examined (Allender, Richardson, Woodhouse, Heard, & Brain, 2000).

In this paper, a novel CL sensor for determination of SMZ using CG-MIP as recognition was developed. The CG-MIP of SMZ was synthesized, chitosan/grapheme oxide was used for improving the adsorption capacity. The surface morphology and adsorption performance of CG-MIP were studied. According to the results, the CG-MIP was suitable for using in CL sensor. The sensor was reusable and successfully used in determining of SMZ in drug samples with advantages of molecularly imprinted, chemiluminescence. Under the optimal conditions, as expected the SMZ-CG-MIP-CL sensor showed very high sensitivity and selectivity to SMZ.

2. Experimental

2.1. Materials and reagents

Sulfamethoxazole (SMZ) was purchased from Shanghai Jingchun Reagent Factory; acrylamide (AM) was purchased from Tianjin Chemical Reagent Co., Ltd; ethylene glycol dimethacrylate (EGDMA) were supplied from Aladdin Reagent Co., Ltd; 2,2-azobisisobutyronitrile (AIBN) were supplied from Sigma–Aldrich. Chitosan (CS) was obtained from Sinopharm Chemical Reagent Co. Ltd.

The EGDMA was distilled to remove inhibitors. AIBN was recrystallized prior to its use.

The SMZ stock solution (1.0×10^{-2} mol/L), luminol stock solution (1.0×10^{-2} mol/L) and potassium permanganate stock solution (1×10^{-3} mol/L) were prepared and stored in refrigerator, respectively. The methanol, acetic acid, sodium hydroxide, and all the other chemicals were of analytical reagent grade and obtained from Tianjin Chemical Co., Ltd. Double distilled water was used throughout the work.

2.2. Apparatus

The schematic diagram of system used in this study is shown in Fig. 1. The IFFM-E flow injection CL analyzer (Xi'an Remex Electronic Instrument High-Tech Ltd., China) was equipped with an automatic injection system and a detection system. PTFE tube (0.8 mm i.d.) was used to connect all of the components in the flow system. 50 mg CG-MIP particles were packed into a Y-shape colorless tube (5 mm × 5 cm i.d. length) which was served as a flow cell. Both ends of the tube were stuffed with a small amount of glass wool. The tube was placed in front of the photomultiplier and connected with the flow system. The CG-MIP flow cell must be conditioned prior to its first time use. The CL signal was analyzed with a computer (Fang et al., 2009).

2.3. Preparation of SMZ-CG-MIP

Graphene oxide nanosheets were prepared according to the reported before (Chun et al., 2011), Graphite oxide was prepared from nature graphite powders by a modified Hummers method (Hummers & Offeman, 1958). Firstly, 120 mL H_2SO_4 (95%) was added into a 500 mL flask, and then cooled by immersion in an ice bath followed by stirring. Subsequently, 5.0 g graphite powder and 2.5 g $NaNO_3$ were added under vigorous stirring to avoid agglomeration. After the graphite powder was well dispersed, 15 g $KMnO_4$ was added gradually under stirring and the temperature of the mixture was kept to be below 10 °C by cooling. The ice bath was then removed and the mixture was stirred at room temperature overnight. As the reaction progressed, the mixture gradually became pasty and the color turned into light brownish. Secondly, 150 mL of H_2O was slowly added to the paste with vigorous agitation. Because the addition of water in concentrated sulfuric acid medium released a large amount of heat, the addition of water was performed in an ice bath to keep the temperature below 100 °C. The diluted suspension was stirred at 98 °C for 1 day. Then, 50 mL of 30% H_2O_2 was added to the mixture. Finally, the mixture was filtered and washed with 5% HCl aqueous solution to remove metal ions followed by water until the pH was 7. After filtration and drying at 65 °C under vacuum, graphite oxide was obtained as gray powder. Graphene oxide was prepared according to the literature method (Li, Muller, Gilje, Kaner, & Wallace, 2008; Yang et al., 2009). Graphite oxide powders were dispersed in water to create a 0.05 wt% of dispersion. Exfoliation of graphite oxide to GO was achieved by ultrasonication (200 W, 40 kHz) for 1 h, in which the bulk graphite oxide powders were transformed into GO sheets (Jili, Song, Xiaoping, & Lei, 2010; Nakajima, Mabuchi, & Hagiwara, 1988; Zhenglong, Xujing, Junjie, Hongting, & Yongsheng, 2010). The obtained brown dispersion was then subjected to 30 min of centrifugation at 3000 rpm to remove any unexfoliated GO (usually present in a very small amount). The final products were then centrifuged, washed with water, and finally air-dried.

A desired amount of GO powder (0.10–0.30 g) was dispersed into 100 mL of ultrapure water and was treated by mild ultrasound for 15 min in a 250 mL beaker, and there forms a homogeneous suspension. 1 mL HAc and 1.5 g chitosan were added into the suspension sequentially under stirring for 60 min (Donglin et al., 2011).

In a typical experiment (Ying et al., 2010), 1.0 g of CG was dispersed in 100.0 mL of $SOCl_2$ and 20.0 mL of benzene. The mixture was stirred for 24 h under 70 °C at reflux. The obtained solid (CG-CL) was washed with ultra-dried tetrahydrofuran (THF) three times and dried under vacuum at 25 °C. In the next step, 0.5 g CG-CL, 2.0 mL 2-hydroxylethyl-2′-bromoisobutyrate ($HOCH_2$-$CH_2OCOC(CH_3)_2Br$, HEBrIB) and 20.0 mL anhydrous toluene was mixed under nitrogen protection followed by added 0.5 mL anhydrous triethylamine. The mixture was refluxed for 48 h. The solid was separated by filtration and then washed with ethanol and ether, and vacuum-dried for 12 h to yield CG-Br. Subsequently, 14.5 mL phenyl magnesium bromide was dispersed in 130.0 mL THF, and then 3.5 mL CS_2 was added drop wise. After stirring for 2 h, 1.0 g CG-Br was added under nitrogen protection at 60 °C for 64 h. The reaction was stopped by adding ice hydrochloric acid (1 M, 50.0 mL). The obtained product (C_6H_5-C(S)-S-COO-$(CH_2)_2$-CG) was washed with distilled water three times, and then washed with ether three times.

Subsequently, 0.1 mmol SMZ and 0.4 mmol AM were dispersed into acetone solution, and the mixture was stirred for 1 h. After sealing, shaking, and purging, C_6H_5-C(S)-S-COO-$(CH_2)_2$-CG was added in the mixture, then 2.0 mmol EGDMA, and 15 mg AIBN was added under nitrogen protection at 65 °C for 18 h. The polymerization was stopped by freezing. The obtained product separately washed three times with methanol–acetic acid (9:1, v/v) solution to remove the catalyst and unreacted reagents. Finally, CG-MIP was dried under vacuum at room temperature for 24 h. The chitosan/graphene oxide-molecularly non-imprinted polymers (CG-NIP) was prepared and processed in the same way, but in the absence of any template.

2.4. Adsorption tests

The two groups of same concentration of SMZ standard solution were prepared, CG-MIP and CG-NIP were added into the solution for adsorption under the same conditions. The same volumes of solutions were taken for test at different times to get the adsorption capacity.

A series of different concentrations of standard solution were prepared, and the same qualities CG-MIP were added into the solutions respectively for completely adsorption. The adsorption capacity of CG-MIP was got by chemiluminescence test, according to Langmuir isotherm equation, theory adsorption capacity of CG-MIP was obtained.

2.5. Preparation of MIP for comparative adsorption study

The preparation of MIP for SMZ was as follows: a 25 mL acetone solution containing 0.1 mmol SMZ, 0.4 mmol AM was prepared. After degassing and nitrogen purging for about 5 min to remove oxygen which inhibits the polymerization, the solution was placed at 25 °C for 12 h. Then 2.0 mmol EGDMA and 20 mg AIBN were added into the solution which was continued for 24 h at 60 °C. The polymers were extracted with methanol/acetic acid (9/1, v/v) overnight and washed with distilled water to remove any non-grafted polymer, monomer, residual initiator and the template.

The two different polymers were added into the SMZ solutions for adsorption under the same conditions. After fully adsorption, the precipitate was isolated by centrifugation and the supernatant was tested by flow injection chemiluminescence. Adsorption capacity was obtained according to the regression equation.

2.6. Procedure for the determination of SMZ

The schematic diagram for the SMZ-CG-MIP-CL sensor was shown in Fig. 1 and the determination could be summarized as six steps as follows:

Firstly, Pump 2 was turned on, sample solution was delivered to flow through the CG-MIP column and SMZ in the sample solution was selectively adsorbed on the polymer.

Secondly, Pump 2 pumped continuously ultrapure water to flow through the CG-MIP column to remove the other substances except SMZ.

Thirdly, Pump 2 was stopped and Pump 1 was turned on, the merged stream of luminol, $KMnO_4$ and NaOH flowed through the CG-MIP column to react with SMZ adsorbed in the CG-MIP to produce CL.

Lastly, ultrapure water flowed through the CG-MIP column by pump to clean the CG-MIP for next determination.

3. Results and discussion

3.1. Characterization of GO and CG-MIP

Fourier transform infrared (FTIR) spectra were recorded on a PerkinElmer Spectrum One Spectra by KBr pellet. The nature of the chemical groups on surface of GO and CG-MIP were investigated by FTIR spectra shown in Fig. 2 reveals the presence of the oxygen-containing functional groups. Four bands at 2935, 2495, 1622, 1385 cm^{-1} are the characteristics of benzene ring (C—OH stretching, C—C stretching mode of the sp^2 carbon skeletal network), the peak at 1091 cm^{-1} is characteristic of the C—O—C stretching vibration, which confirms the presence of GO. The peaks located at 1730 and 3419 cm^{-1} correspond to C—O stretching vibrations of the —COOH groups, and O—H stretching vibration, respectively. As shown in CG-MIP, there are two characteristic absorbance bands centered at 1636 and 1597 cm^{-1}, which correspond to the C—O stretching vibration of —NHCO— and the N—H bending of $—NH_2$. However, in the case of GO grafted derivatives, it can be distinctly observed that the NH_2 absorbance band has shifted to a lower value and the intensity of acetylated amino group —NHCO— has increased, which proves that $—NH_2$ groups on the Cs chains have been reacted with the —COOH groups of GO and therefore have been converted to —NHCO— graft points. These indicated that GO was successfully grafted on chitosan. For chitosan, the peaks at 3400 cm^{-1} are corresponding to N—H stretching vibration, of amino group in the spectrum.

The morphological structure of GO and CG-MIP were examined by TEM. TEM images are showed in Fig. 2. From the TEM image, it can be seen that the GO, like wrinkled paper, is very thin and contains some wrinkles. These wrinkles may be important for preventing aggregation of GO and maintaining high surface area. As can be noticed from TEM image of CG-MIP, the almost GO sheets were decorated by the MIP and chitosan films, which indicated that the imprinted sites were generated in the CG-MIP hybrid. We considered that the MIP was stably attached to the CG surface through chemical bonding. And as shown in the figure, MIP was prepared with CG successfully.

X-ray diffraction (XRD) measurements were employed to investigate the phase and structure. As shown in Fig. 3, the XRD pattern of the GO shows a sharp peak at $2\theta = 10.9°$ which is the characteristic peaks of GO. The typical XRD patterns of the CG-MIP composite were showed in the figure. Furthermore, in order to demonstrate the successful formation of surface imprinted polymers, a SEM/EDS analysis showed in Fig. 3, the main elements are H (30.1%), O (29.6%) and C (40.0%), and as seen from the figure, the surface of CG-MIP was rough, compared the smooth surface of GO, the CG-MIP was prepared successfully with recognition sites.

3.2. Adsorption capacity of SMZ-CG-MIP

The effect of time on the adsorption capacity of SMZ was shown in Fig. 4(A). The results demonstrated that the adsorption was rapidly, it was suitable for using in the CG-MIP-CL sensor. The maximum adsorption was 1.89×10^{-5} mol/g. Fig. 4(B) was the

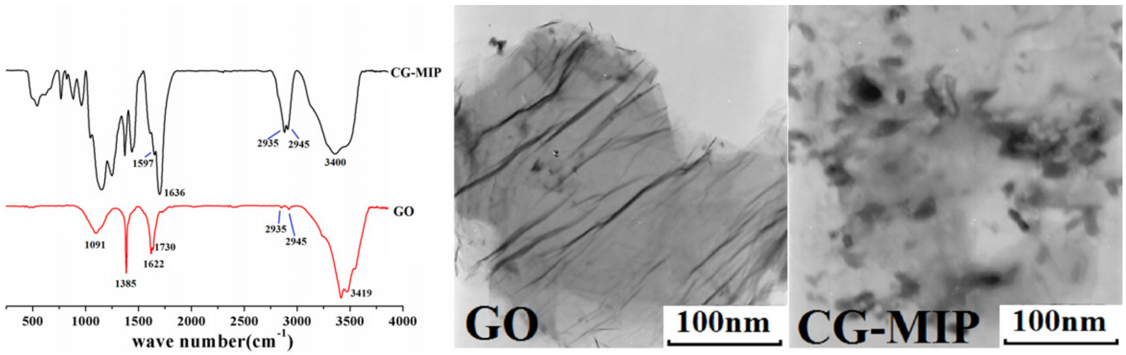

FTIR of GO and CG-MIP

TEM of GO and CG-MIP

Fig. 2. The FTIR and TEM characterization.

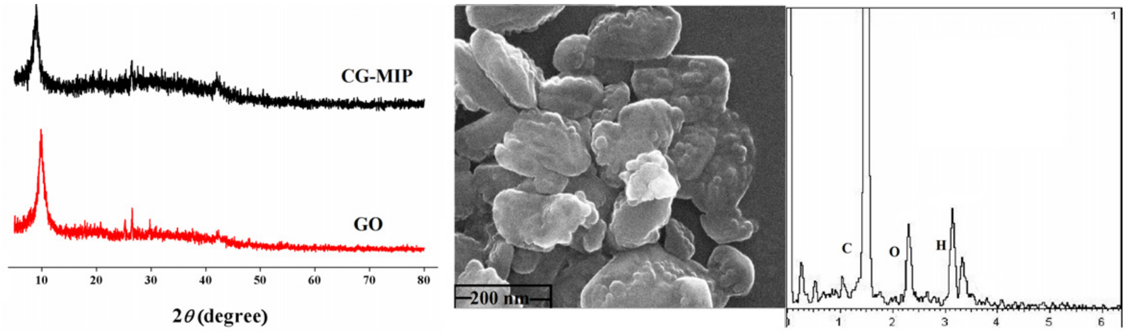

XRD of GO and CG-MIP

SEM of CG-MIP

EDS of CG-MIP

Fig. 3. The XRD, SEM and EDS characterization.

Langmuir's adsorption isotherms of SMZ. The adsorption capacity of SMZ increased with increasing of the SMZ concentration. The theory maximum adsorption capacity of the SMZ obtained by Langmuir isotherm was 1.94×10^{-5} mol/g which was same with the experimental results approximate.

The adsorption capacity of CG-MIP was got by chemiluminescence test, according to Langmuir isotherm equation of Eq. (2), and theory adsorption capacity of CG-MIP was obtained.

$$\frac{c_e}{Q_e} = \frac{c_e}{Q_m} + \frac{1}{Q_m K_L} \tag{2}$$

where c_e is the equilibrium concentration of metal ions in solution (mol/g), Q_e is the adsorbed value of metal ions at equilibrium concentration (mol/g), Q_m is the maximum adsorption capacity (mol/g), and K_L is the Langmuir binding constant, which is related to the energy of adsorption. Plotting c_e/Q_e against c_e gives a straight line with slope and intercept equal to $1/Q_m$ and $1/(K_L Q_m)$, respectively. By calculating, the results were as follows:

$$\frac{c_e}{Q_e} = 5.15 \times 10^4\, c_e + 0.6197, \quad Q_m = 1.94 \times 10^{-5}\ \text{mol/g},$$

$$K_L = 5.15 \times 10^4\ \text{g/mol} \quad (R^2 = 0.9988)$$

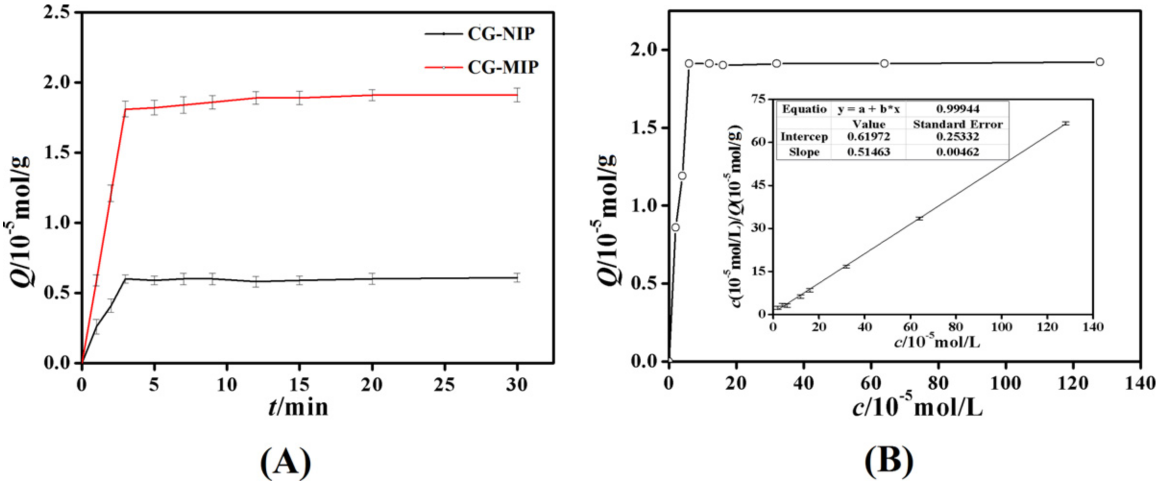

Fig. 4. The adsorption performance of CG-MIP, CG-NIP.

Table 1
Results of recovery tests of SMZ in the drugs sample.

Sample	Accurate, 10^{-4} mol/mL	Measured, 10^{-4} mol/mL	Average, 10^{-4} mol/mL	RSD%	Added, 10^{-4} mol/mL	Found, 10^{-4} mol/mL	Recovery, %	Average, %	RSD%
1#	1.800	1.796	1.799	1.304	1.000	1.030	103.0	101.6	2.442
2#	1.800	1.813			5.000	4.980	99.60		
3#	1.800	1.789			10.00	10.19	101.9		
4#	1.800	1.798			15.00	15.26	101.7		

The theory maximum adsorption capacity of the SMZ obtained by Langmuir isotherm was 1.94×10^{-5} mol/g and was approximate to the experimental result (1.89×10^{-5} mol/g).

3.3. Adsorption comparison of CG-MIP and MIP

The adsorption results are shown in Fig. 5. According to the results, the adsorption capacity of CG-MIP (1.89×10^{-5} mol/g) was much higher than common MIP (0.97×10^{-6} mol/g). The results confirmed that the adding of graphene oxide improving adsorption capacity, the large difference made the CG-MIP more appropriate to use in the CL sensor.

Chitosan exhibits a high adsorption capacity because of its high amino and hydroxyl functional group content. GO has a high specific surface area, molecularly imprinted polymers based on graphene oxide have more recognition sites. As a result, selective adsorption capacity was greatly improved.

3.4. Optimization of SMZ-CG-MIP-CL sensor

The reaction between luminol and potassium permanganate shows weak CL emission and a strong CL emission was recorded when SMZ was injected into the above mixed solution. The peak heights of the CL emission were proportional to the concentration of SMZ (Qiu, Xi, Lu, Fan, & Luo, 2012). The optimization experiment was carried out to get a better knowledge of the CL reaction of luminol–$KMnO_4$–SMZ through the schematic diagram shown in Fig. 1.

With the luminol concentration in the range from 7.0×10^{-5} to 3×10^{-3} mol/L, the CL intensity increased with raising the concentration of luminol up to 2.0×10^{-4} mol/L. Above 2.0×10^{-4} mol/L, the CL intensity decreased. Thus, the 2.0×10^{-4} mol/L luminol was used for further work.

The effect of sodium hydroxide concentration as medium was examined over 1×10^{-4} to 2×10^{-2} mol/L range, and the CL intensity reached up to maximum value when 3×10^{-3} mol/L concentration of sodium hydroxide. But higher concentration of sodium hydroxide lowered the CL intensity of this system.

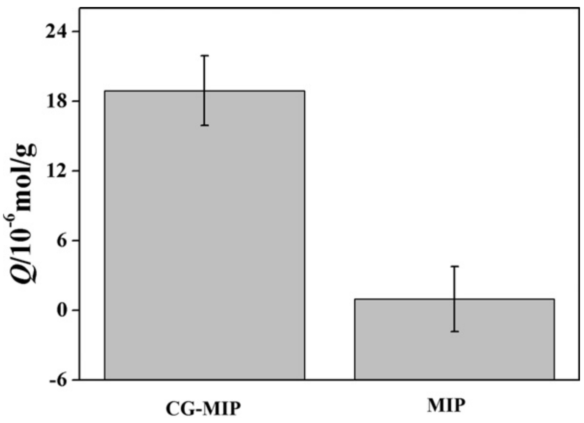

Fig. 5. Adsorption comparison of CG-MIP and MIP.

The effect of potassium permanganate concentration was examined from 1.0×10^{-4} to 1.2×10^{-3} mol/L, the CL intensity reached maximum when potassium permanganate was 4.0×10^{-4} mol/L.

In this work, the experiments were finished according to the schematic diagram shown in Fig. 1. The adsorption time for SMZ is a very important parameter for the amount of SMZ absorbed on the CG-MIP, the adsorption time depends on peristaltic pumps speed. The relation of CL intensity with the pumps speed was observed under the condition that 10–50 rpm. It was observed that the CL intensity reached maximum at 15 rpm. According to experiments, too small pumps speed made other substances adsorbed by CG-MIP at a time. SMZ molecules cannot adsorb by CG-MIP completely under too large pumps speed. So the 15 rpm pumps speed was chosen for the determination with good results.

3.5. The analytical performance for the CG-MIP-CL sensor

Under optimal conditions, the CL intensity responded linearly to the concentration of SMZ within 1.0×10^{-7} mol/L to 2.3×10^{-3} mol/L with a detection limit of 2.9×10^{-8} mol/L (3σ), which is lower than that of conventional methods. The relative standard deviation (*RSD*) for the determination of 4.0×10^{-4} mol/L SMZ was 1.92% ($n = 11$). The regression equation is $I_{CL} = -279.7 + 3.641 \times 10^6 c$ (c being the SMZ concentration (10^{-4} mol/L)) with a correlation coefficient of 0.9989.

3.6. SMZ-CG-MIP-CL sensors measuring samples

Under the selected conditions, following the described procedures, the proposed method was applied to determination of SMZ in drugs samples. All the results are listed in Table 1. The results indicated that the SMZ-CG-MIP-CL sensor could detect the SMZ in the samples without sample purification step. The recoveries for

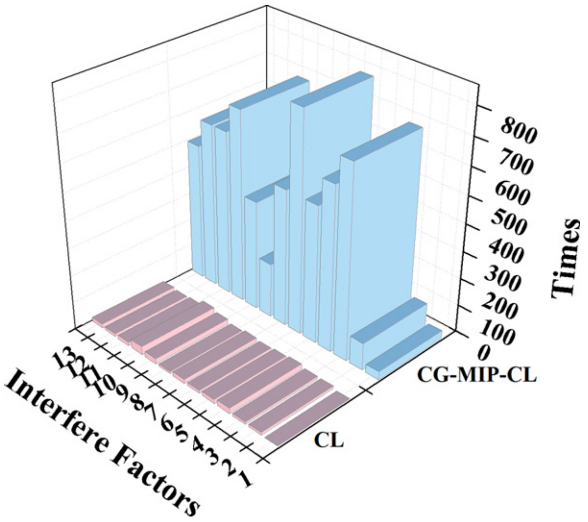

Fig. 6. The tolerable ratio of interfering species to SMZ. 1: Sulfonamides pyrimidine; 2: Ag^+; 3: Cu^{2+}; 4: Fe^{2+}; 5: Ce^{3+}; 6: b-cyclodextrins; 7: Pd^{2+}; 8: Ba^{2+}; 9: K^+; 10: Na^+; 11: Mg^{2+}; 12: Cd^{2+}; 13: Ca^{2+}.

different concentration levels varied from 99.6% to 103%. So the SMZ-CG-MIP-CL sensor for the determination of SMZ is very useful.

3.7. Interferences study

Under the optimum conditions, the factors which may interfere potentially the determination of SMZ were investigated. The relative error was controlled within ±5.00% and the tolerance ratios with or without CG-MIP as Fig. 6. The CG-MIP-CL sensor has higher selectivity than CL analysis.

4. Conclusions

In this work, the preparation and application of CL sensor by using the SMZ-CG-MIP as recognition element was described, and the high selectivity and sensitivity of SMZ-CG-MIP was obtained, and the possible mechanism was also demonstrated. The CG-MIP was synthesized using chitosan/graphene oxide which improved the adsorption capacity. Due to the special binding sites on the CG-MIP, the SMZ could be absorbed by the CG-MIP selectively and the special binding property improved the selectivity and sensitivity of the CL analysis. From this point of view, the CG-MIP-CL sensor was developed and applied to determinate the SMZ in drugs samples directly. Since the CG-MIP could get rid of the interferences effectively, the obtained SMZ-CG-MIP-CL sensor has shown to provide a sensitive and fast method for on-line determination of SMZ and with satisfactory results.

Acknowledgements

This work was supported by the Shandong Provincial Natural Science Foundation of China (Nos. ZR2012BM020, ZR2012BQ018) and the Scientific and technological development Plan Item of Jinan City in China (No. 201202088).

References

Allender, C. J., Richardson, C., Woodhouse, B., Heard, C. M., & Brain, K. R. (2000). Pharmaceutical applications for molecularly imprinted polymers. *International Journal of Pharmaceutics*, *195*, 39–43.

Chun, W., Cheng, F., Yongjun, G., Xiaoxing, M., Qiuhua, W., & Zhi, W. (2011). Preparation of a graphene-based magnetic nanocomposite for the removal of an organic dye from aqueous solution. *Chemical Engineering Journal*, *173*, 92–97.

Donglin, H., Lifeng, Y., Wufeng, C., & Wan, L. (2011). Preparation of chitosan/graphene oxide composite film with enhanced mechanical strength in the wet state. *Carbohydrate Polymers*, *83*, 653–658.

Du, J. X., Shen, L. H., & Lu, J. R. (2003). Flow injection chemiluminescence determination of epinephrine using epinephrine-imprinted polymer as recognition material. *Analytica Chimica Acta*, *489*, 183–189.

Englert, J. M., Rö hrl, J., Schmidt, C. D., Graupner, R., Hundhausen, M., & Hauke, F. (2009). Soluble graphene: Generation of aqueous graphene solutions aided by a perylenebisimide-based bolaamphiphile. *Advanced Materials*, *21*, 4265–4269.

Fang, Y., Yan, S., Ning, B., Liu, N., Gao, Z., & Chao, F. (2009). Flow injection chemiluminescence sensor using molecularly imprinted polymers as recognition element for determination of maleic hydrazide. *Biosensors & Bioelectronics*, *24*, 2323–2327.

Hummers, J. W. S., & Offeman, R. E. (1958). Preparation of graphitic oxide. *Journal of the American Chemical Society*, *80*, 1339.

Jili, W., Song, B., Xiaoping, S., & Lei, J. (2010). Preparation and characterization of graphene/CdS nanocomposites. *Applied Surface Science*, *257*, 747–751.

Li, D., Muller, M. B., Gilje, S., Kaner, R. B., & Wallace, G. G. (2008). Processable aqueous dispersions of graphene nanosheets. *Nature Nanotechnology*, *3*, 101–105.

Luaces, M. D., Martínez, N. C., Granda, M., Valdés, A. C., Pérez-Conde, C., & Gutiérrez, A. M. (2011). A novel flow injection chemiluminescence determination of Cr(VI) with Dichlorotris (1,10-phenanthroline) ruthenium(II). *Talanta*, *85*, 1904–1908.

Mahony, J. O., Nolan, K., Smyth, M. R., & Mizaikoff, B. (2005). Molecularly imprinted polymers-potential and challenges in analytical chemistry. *Analytica Chimica Acta*, *534*, 31–39.

Mingyu, Y., Minchien, H., Shuhang, L., Poi, L., Hanmin, T., & Chenchi, M. (2011). Preparation of graphene/multi-walled carbon nanotube hybrid and its use as photoanodes of dye-sensitized solar cells. *Carbon*, *49*, 3597–3606.

Mosbach, K. (1994a). Similarities between a soybean nodulin, Neurospora crassa sulphate permease II and a putative human tumour suppressor. *Trends in Biochemical Sciences*, *19*, 19.

Mosbach, K. (1994b). Molecular imprinting. *Trends in Biochemical Sciences*, *19*, 9–14.

Mosbach, K., & Ramstr̈om, O. (1996). The emerging technique of molecular imprinting and its future impact on biotechnology. *Nature Biotechnology*, *14*, 163–170.

Nakajima, T., Mabuchi, A., & Hagiwara, R. (1988). A new structure model of graphite oxide. *Carbon*, *26*, 357–361.

Novoselov, K. S., Geim, A. K., Morozov, S. V., Jiang, D., Zhang, Y., & Dubonos, S. V. (2004). Electric field effect in atomically thin carbon films. *Science*, *306*, 666–669.

Park, S., An, J. H., Piner, R. D., Jung, I., Yang, Z., & Velamakanni, A. (2008). Aqueous suspension and characterization of chemically modified graphene sheets. *Chemistry of Materials*, *20*, 6592–6594.

Qiu, H., Xi, Y., Lu, F., Fan, L., & Luo, C. (2012). Determination of l-phenylalanine online based on molecularly imprinted polymeric microspheres and flow injection chemiluminescence. *Spectrochimica Acta Part A*, *86*, 456–460.

Shea, K. J. (1994). Molecular imprinting of synthetic network polymers: The de novo synthesis of macromolecular binding and catalytic sites. *Trends in Polymer Science*, *2*, 166–173.

Stankovich, S., Dikin, D. A., Dommett, G. H. B., Kohlhaas, K. M., Zimney, E. J., & Stach, E. A. (2006). Graphene-based composite materials. *Nature*, *442*, 282–286.

Steinke, J., Sherrington, D. C., & Dunkin, I. R. (1995). Imprinting of synthetic polymers using molecular templates. *Advances in Polymer Science*, *123*, 81–125.

Veca, L. M., Lu, F. S., Meziani, M. J., Cao, L., Zhang, P. Y., & Qi, G. (2009). Polymer functionalization and solubilization of carbon nanosheets. *Chemical Communications*, *18*, 2565–2567.

Wulff, G. (1995). Molecular imprinting in cross-linked materials with the aid of molecular templates—a way towards artificial antibodies, *Angewandte Chemie. International Edition in English*, *34*, 1812–1832.

Wulff, G., Heide, B., & Helfmeier, G. (1986). Molecular recognition through the exact placement of functional groups on rigid matrices via a template approach. *Journal of the American Chemical Society*, *108*, 1089–1091.

Yan, M., Yu, B., Shiyu, G., Fenghua, L., & Li, N. (2011). Electrochemical sensor for dopamine based on a novel graphene-molecular imprinted polymers composite recognition element. *Biosensors & Bioelectronics*, *28*, 291–297.

Yang, H. F., Li, F. H., Shan, C. S., Han, D. X., Zhang, Q. X., & Niu, L. (2009). Covalent functionalization of chemically converted graphene sheets via silane and its reinforcement. *Journal of Materials Science*, *19*, 4632–4638.

Ying, L., Xin, L., Cunku, D., Jingyao, Q., & Xijiang, H. (2010). A graphene oxide-based molecularly imprinted polymer platform for detecting endocrine disrupting chemicals. *Carbon*, *48*, 3427–3433.

Zeng, H. J., Yang, R., Wang, Q. W., Li, J. J., & Qu, L. B. (2011). Determination of melamine by flow injection analysis based on chemiluminescence system. *Food Chemistry*, *127*, 842–846.

Zhenglong, Y., Xujing, S., Junjie, Y., Hongting, P., & Yongsheng, L. (2010). Preparation of poly(3-hexylthiophene)/graphene nanocomposite via in situ reduction of modified graphite oxide sheets. *Applied Surface Science*, *257*, 138–142.